文章编号:1000-0887(2012)08-0974-14



# 滑移和感应磁场对 Johnson-Segalman 流体蠕动传输的影响*

T·哈亚特[1], K·诺琳[2], A·艾尔萨额蒂[3]

(1. 真纳大学 数学系 45320,伊斯兰堡 44000,巴基斯坦;
2. COMSATS 信息技术学院 数学系,阿托克 43600,巴基斯坦;
3. 阿卜杜勒-阿齐兹国王大学 科学学院 数学系,吉达 21589,沙特阿拉伯)

**摘要:** 存在感应磁场和滑移条件下,研究 Johnson-Segalman(J-S)流体在平面通道中的蠕动流.通道中的流动认为是对称的,并在剪切应力项中考虑了速度的滑移条件.首先给出问题的数学公式,然后在长波长和低 Reynolds 数近似下,求解该方程组得到摄动解,确定沿管道截面的压力增量、轴向速度、微转动分量、流函数、磁力函数、轴向感应磁场和电流密度分布公式.导出了小数值 Weissenberg 数时解的表达式,分析并勾画出诸流动物理量的有趣变化.

**关 键 词:** 感应磁场; 滑移条件; Johnson-Segalman 流体
**中图分类号:** O357.2 **文献标志码:** A
DOI: 10.3879/j.issn.1000-0887.2012.08.006

## 引 言

显然,流体在通道/管道中,在给定边界上产生的流动动力学,很容易用一个行波来描述蠕动的进程.这样的蠕动进程在生理流体的输送中扮演着关键角色,如血液的体外循环、尿液从肾脏到膀胱的传输、食糜在胃肠道中的输送、精子进入子宫颈管道、卵子游入输卵管、男性腹腔中生殖器官的输出小管等.如细胞分离器、关节泵、指针和滚子泵、心肺机这样的器具,都是在这个进程下运转的.自从 Latham[1] 和 Shapiro 等[2] 的开创性工作以来,通过大量的理论、计算和试验努力,推进了在不同情况下对粘性非 Newton 流体蠕动流的理解.一些最新的、可能提及求解粘性非 Newton 流体蠕动流问题的研究可以参看文献[3-20].

早期的研究表明,没有掌握住无滑移条件,关于非 Newton 流体蠕动流有用的信息就少得可怜.Ebaid[21] 就粘性流体在对称通道中的流动,报道了壁面滑移和感应磁场对蠕动流的影响.Srinivas 等[22] 研究了滑移条件和壁面特性,对粘性流体 MHD 蠕动传输的影响,在他们的流动分析中,还讨论了热的传输问题.Mandviwalla 和 Archer[23] 在有滑移条件下,理论上分析了矩形通道中蠕动泵的传输问题.El-Shehawy 等[24] 研究了 Maxwell 流体在有滑移影响时的蠕动流.

* **收稿日期:** 2011-01-04; **修订日期:** 2012-04-25
**基金项目:** 巴基斯坦高等教育委员会(HEC)资助项目(074-2997-$P_S$4-021)
**作者简介:** T. Hayat(联系人. Tel: +92-51-90642172; Fax: +92-51-2601171; E-mail: pensy_t@yahoo.com).
本文原文为英文,黄锋 译,张禄坤 校.

Sobh[25]在均匀的和非均匀的通道中,讨论了滑移速度对耦合应力流体蠕动流的影响. Hayat 等[26]在多孔介质中研究了局部滑移对蠕动流的影响. Ali 等[27]报道了局部滑移和可变粘度对通道中 MHD 粘性流体蠕动流的影响. Hayat 等[28]在二维通道中,验证了局部滑移和传热对粘性流体蠕动流的组合影响. 在另一文献中,Hayat 等[29]在对称通道中,分析了滑移对三阶流体蠕动运动的影响.

另一方面,感应磁场对蠕动运动的影响没有予以足够重要的关注. Vishnyakov 和 Pavlov[30]首先就 Newton 流体的感应磁场问题进行了研究. 随后, Mekheimer[31]在对称通道中导电耦合应力流体的 MHD 流动问题进行了分析. 最近,Nadeem 和 Akram[32]尝试将同样的理论结果推广到非对称通道. Hayat 等[33-34]在感应磁场影响下的对称通道中,分别得到了不可压缩三阶流体和 Carreau 流体的解析解. Mekheimer[35]分析了有感应磁场存在时不可压缩磁微极流体的流动.

本文的目的是就滑移和感应磁场,对非 Newton 流体在通道中蠕动传输时的组合影响进行研究. 建立起 Johnson-Segalman 流体本构方程可供应用的数学模型,还允许发展到非均匀变形,从这个意义上来说,考虑这个流体模型是十分重要的. 过去,不同的研究者为了描述流体的喷射现象使用过这个模型,特别是出现在非 Newton 流体的流动之中,在一个临界压力梯度下,推进压力梯度小的增长,使体积有大的增长. 通过图形分析了感兴趣参数的不同特性. 本文的结构组织如下:第 1 节中给出了问题的公式,第 2 节中给出了小数值 Weissenberg 数下的级数表达式,第 3 节就蠕流泵和俘获现象、流动和磁场特性进行了讨论.

## 1　问题的公式化

考虑不可压缩 Johnson-Segalman 流体,在二维通道中作磁流体动力学流动. 在 Cartesian 坐标系 $(\bar{X},\ \bar{Y})$ 中,选取 $\bar{X}$ 轴为波的传播方向,$\bar{Y}$ 轴垂直于 $\bar{X}$ 轴. 强度为 $H_0$ 的恒定磁场作用于 $\bar{Y}$ 方向. 由其产生的感应磁场为 $\boldsymbol{H}(\bar{h}_{\bar{x}}(\bar{X},\ \bar{Y},\ \bar{t}),\ \bar{h}_{\bar{y}}(\bar{X},\bar{Y},\ \bar{t}),\ 0)$,因此,总磁场可以表示为 $\boldsymbol{H}^{+}\ (\bar{h}_{\bar{x}}(\bar{X},\ \bar{Y},\ \bar{t}),\ H_0 + \bar{h}_{\bar{y}}(\bar{X},\bar{Y},\bar{t}),0)$ . 壁面条件表示为

$$\bar{h}(\bar{X},\bar{t}) = a + b\sin\left(\frac{2\pi}{\lambda}(\bar{X} - c\bar{t})\right), \tag{1}$$

其中, $a$ 为通道半宽度,$b$ 为波幅,$\lambda$ 为波长,$c$ 为波速,$\bar{t}$ 为时间.

取适当的速度场 $\boldsymbol{V}$ 为

$$\boldsymbol{V} = [\bar{U}(\bar{X},\bar{Y},\bar{t}),\bar{V}(\bar{X},\bar{Y},\bar{t}),0]. \tag{2}$$

流动的控制方程给出如下:

连续方程

$$\nabla\cdot\boldsymbol{V} = 0. \tag{3}$$

动量方程

$$\rho\frac{\mathrm{d}\boldsymbol{T}}{\mathrm{d}t} = \mathrm{div}\boldsymbol{T} + \mu_e(\nabla\times\boldsymbol{H}^{+})\times\boldsymbol{H}^{+} =$$

$$\mathrm{div}\boldsymbol{T} + \mu_e\left[(\boldsymbol{H}^{+}\cdot\nabla)\boldsymbol{H}^{+} - \frac{\nabla\boldsymbol{H}^{+2}}{2}\right]. \tag{4}$$

Maxwell 方程

$$\nabla\cdot\boldsymbol{E} = 0,\ \nabla\cdot\boldsymbol{H} = 0, \tag{5}$$

$$\nabla\times \boldsymbol{E} = -\mu_e \frac{\partial \boldsymbol{H}}{\partial t},\ \nabla\times \boldsymbol{H} = \boldsymbol{J}, \tag{6}$$

这里,没有考虑位移电流,且

$$\boldsymbol{J} = \sigma(\boldsymbol{E} + \mu_e(\boldsymbol{V}\times \boldsymbol{H}))\,. \tag{7}$$

感应磁场方程

$$\frac{\mathrm{d}\boldsymbol{H}^+}{\mathrm{d}t} = \nabla\times(\boldsymbol{V}\times \boldsymbol{H}^+) + \frac{1}{\zeta}\nabla^2\boldsymbol{H}^+\,. \tag{8}$$

对应于 Johnson-Segalman 流体模型的本构关系为

$$\boldsymbol{T} = -p\bar{\boldsymbol{I}} + \bar{\boldsymbol{\tau}}, \tag{9}$$

$$\bar{\boldsymbol{\tau}} = 2\mu\bar{\boldsymbol{D}} + \bar{\boldsymbol{S}}, \tag{10}$$

$$\bar{\boldsymbol{S}} + m\left[\frac{\mathrm{d}\boldsymbol{S}}{\mathrm{d}t} + \bar{\boldsymbol{S}}(\bar{\boldsymbol{W}} - e\bar{\boldsymbol{D}}) + (\bar{\boldsymbol{W}} - e\bar{\boldsymbol{D}})^{\mathrm{T}}\bar{\boldsymbol{S}}\right] = 2\eta\bar{\boldsymbol{D}}, \tag{11}$$

$$\bar{\boldsymbol{D}} = \frac{1}{2}(\bar{\boldsymbol{L}} + \bar{\boldsymbol{L}}^{\mathrm{T}}),\ \bar{\boldsymbol{W}} = \frac{1}{2}(\bar{\boldsymbol{L}} + \bar{\boldsymbol{L}}^{\mathrm{T}}),\ \bar{\boldsymbol{L}} = \mathrm{grad}\bar{\boldsymbol{V}}\,. \tag{12}$$

这里,$\mu_e$ 为磁渗透率,$\boldsymbol{J}$ 为电流密度,$\sigma$ 为电导率,$\boldsymbol{E}$ 为电场,$\boldsymbol{H}$ 为磁场,$\zeta = \sigma\mu_e$ 为磁扩散率,$\boldsymbol{T}$ 为 Cauchy 应力张量,$\bar{\boldsymbol{\tau}}$ 为附加应力张量,$p$ 为压力,$\bar{\boldsymbol{I}}$ 为单位张量,$\mu$ 和 $\eta$ 为粘度系数,$m$ 为松弛时间,$\bar{\boldsymbol{D}}$ 和 $\bar{\boldsymbol{W}}$ 为分别为速度梯度的对称和反对称部分,$\mathrm{d}/\mathrm{d}t$ 为随体导数,$e$ 为滑移参数. 当 $m = 0 = \mu$ 时,本文的流体模型简化为经典的 Navier-Stokes 模型;进一步地,$e = 1$ 和 $\mu = 0$ 时,其简化为 Maxwell 模型.

通过利用下面的表达式,将实验室坐标系 $(\bar{X},\bar{Y})$ 中的非稳定流动,转变为波动坐标系 $(\bar{x},\bar{y})$ 中的稳定流动:

$$\begin{cases}\bar{x} = \bar{X} - c\bar{t},\ \bar{y} = \bar{Y},\\ \bar{u}(\bar{x},\bar{y}) = \bar{U} - c,\ \bar{v}(\bar{x},\bar{y}) = \bar{V},\end{cases} \tag{13}$$

其中,$(\bar{U},\bar{V})$ 和 $(\bar{u},\bar{v})$ 分别表示实验室坐标系和波动坐标系中的速度分量.

应用方程(3)~(13),可以得到

$$\frac{\partial\bar{u}}{\partial\bar{x}} + \frac{\partial\bar{v}}{\partial\bar{y}} = 0, \tag{14}$$

$$\rho\left(\bar{u}\frac{\partial}{\partial\bar{x}} + \bar{v}\frac{\partial}{\partial\bar{y}}\right)\bar{u} + \frac{\partial\bar{p}}{\partial\bar{x}} = \mu\left(\frac{\partial^2}{\partial\bar{x}^2} + \frac{\partial^2}{\partial\bar{y}^2}\right)\bar{u} + \frac{\partial\bar{S}_{xx}}{\partial\bar{x}} + \frac{\partial\bar{S}_{xy}}{\partial\bar{y}} - \frac{\mu_e}{2}\left(\frac{\partial\boldsymbol{H}^{+2}}{\partial\bar{x}}\right) + \mu_e\left(\bar{h}_{\bar{x}}\frac{\partial\bar{h}_x}{\partial\bar{x}} + \bar{h}_{\bar{y}}\frac{\partial\bar{h}_x}{\partial\bar{y}} + H_0\frac{\partial\bar{h}_x}{\partial\bar{y}}\right), \tag{15}$$

$$\rho\left(\bar{u}\frac{\partial}{\partial\bar{x}} + \bar{v}\frac{\partial}{\partial\bar{y}}\right)\bar{v} + \frac{\partial\bar{p}}{\partial\bar{y}} = \mu\left(\frac{\partial^2}{\partial\bar{x}^2} + \frac{\partial^2}{\partial\bar{y}^2}\right)\bar{v} + \frac{\partial\bar{S}_{xy}}{\partial\bar{x}} + \frac{\partial\bar{S}_{yy}}{\partial\bar{y}} - \frac{\mu_e}{2}\left(\frac{\partial\boldsymbol{H}^{+2}}{\partial\bar{y}}\right) +$$

$$\mu_e\left(\bar{h}_{\bar{x}}\frac{\partial \bar{h}_{\bar{y}}}{\partial \bar{x}}+\bar{h}_{\bar{y}}\frac{\partial \bar{h}_{\bar{y}}}{\partial \bar{y}}+H_0\frac{\partial \bar{h}_{\bar{y}}}{\partial \bar{y}}\right), \tag{16}$$

$$2\eta\frac{\partial \bar{u}}{\partial \bar{x}}=\bar{S}_{xx}+m\left(\bar{u}\frac{\partial}{\partial \bar{x}}+\bar{v}\frac{\partial}{\partial \bar{y}}\right)\bar{S}_{xx}-2em\bar{S}_{xx}\frac{\partial \bar{u}}{\partial \bar{x}}+m\left((1-e)\frac{\partial \bar{v}}{\partial \bar{x}}-(1+e)\frac{\partial \bar{u}}{\partial \bar{y}}\right)\bar{S}_{xy}, \tag{17}$$

$$\eta\left(\frac{\partial \bar{u}}{\partial \bar{y}}+\frac{\partial \bar{v}}{\partial \bar{x}}\right)=\bar{S}_{xy}+m\left(\bar{u}\frac{\partial}{\partial \bar{x}}+\bar{v}\frac{\partial}{\partial \bar{y}}\right)\bar{S}_{xy}+\frac{m}{2}\left((1-e)\frac{\partial \bar{u}}{\partial \bar{y}}-(1+e)\frac{\partial \bar{v}}{\partial \bar{x}}\right)\bar{S}_{xx}+\frac{m}{2}\left((1-e)\frac{\partial \bar{v}}{\partial \bar{x}}-(1+e)\frac{\partial \bar{u}}{\partial \bar{y}}\right)\bar{S}_{yy}, \tag{18}$$

$$2\eta\frac{\partial \bar{v}}{\partial \bar{y}}=\bar{S}_{yy}+m\left(\bar{u}\frac{\partial}{\partial \bar{x}}+\bar{v}\frac{\partial}{\partial \bar{y}}\right)\bar{S}_{yy}-2em\bar{S}_{yy}\frac{\partial \bar{v}}{\partial \bar{y}}+m\left((1-e)\frac{\partial \bar{u}}{\partial \bar{y}}-(1+e)\frac{\partial \bar{v}}{\partial \bar{x}}\right)\bar{S}_{xy}. \tag{19}$$

利用下面的定义式：

$$\begin{cases} We=\dfrac{mc}{a},\ x=\dfrac{\bar{x}}{\lambda},\ y=\dfrac{\bar{y}}{s},\ t=\dfrac{c\bar{t}}{\lambda},\ p=\dfrac{a^2\bar{p}}{c\lambda(\mu+\eta)}, \\ \delta=\dfrac{a}{\lambda},\ S=\dfrac{a\bar{S}}{\eta c},\ u=\dfrac{\bar{u}}{c},\ v=\dfrac{\bar{v}}{c},\ Re=\dfrac{ca\rho}{\eta},\ Rm=\sigma\mu_e ac, \\ S=\dfrac{H_0}{c}\sqrt{\dfrac{\mu_e}{\rho}},\ \phi=\dfrac{\bar{\phi}}{H_0 a},\ \bar{h}_{\bar{x}}=\bar{\phi}_{\bar{y}},\ \bar{h}_{\bar{y}}=-\bar{\phi}_{\bar{x}},\ E=\dfrac{-E}{cH_0\mu_e}, \\ p_m=p+\dfrac{1}{2}Re\delta\dfrac{\mu_e \boldsymbol{H}^{+2}}{(\mu+\eta)\rho c^2},\ Ha^2=ReS^2Rm, \end{cases} \tag{20}$$

$$h=\frac{\bar{h}}{a}=1+\alpha\sin(2\pi x), \tag{21}$$

$$u=\frac{\partial \Psi}{\partial y},\ v=-\delta\frac{\partial \Psi}{\partial x},\ h_x=\frac{\partial \phi}{\partial y},\ h_y=-\delta\frac{\partial \phi}{\partial x} \tag{22}$$

将方程(14)～(19)变为

$$Re\delta\left(\frac{\partial \Psi}{\partial y}\frac{\partial}{\partial x}-\frac{\partial \Psi}{\partial x}\frac{\partial}{\partial y}\right)\frac{\partial \Psi}{\partial y}+\left(\frac{\mu+\eta}{\eta}\right)\frac{\partial p_m}{\partial x}=\delta\frac{\partial S_{xx}}{\partial x}+\frac{\partial S_{xy}}{\partial y}+\delta^2\frac{\mu}{\eta}\left(\frac{\partial^3 \Psi}{\partial x^2\partial y}+\frac{\partial^3 \Psi}{\partial y^3}\right)+\delta ReS^2\left(\frac{\partial \phi}{\partial y}\frac{\partial}{\partial x}-\frac{\partial \phi}{\partial x}\frac{\partial}{\partial y}\right)\frac{\partial \phi}{\partial y}+ReS^2\frac{\partial^2 \phi}{\partial y^2}, \tag{23}$$

$$-Re\,\delta^3\left(\frac{\partial \Psi}{\partial y}\frac{\partial}{\partial x}-\frac{\partial \Psi}{\partial x}\frac{\partial}{\partial y}\right)\frac{\partial \Psi}{\partial x}+\left(\frac{\mu+\eta}{\mu}\right)\frac{\partial p_m}{\partial y}=\delta\left(\delta\frac{\partial S_{yx}}{\partial x}+\frac{\partial S_{yy}}{\partial y}\right)-\delta^2\frac{\mu}{\eta}\left(\delta^2\frac{\partial^3 \Psi}{\partial x^3}+\frac{\partial^3 \Psi}{\partial x\partial y^2}\right)-$$

$$\delta^3 ReS^2\left(\frac{\partial\phi}{\partial y}\frac{\partial}{\partial x}-\frac{\partial\phi}{\partial x}\frac{\partial}{\partial y}\right)\frac{\partial\phi}{\partial x}-Re\,\delta^2S^2\,\frac{\partial^2\phi}{\partial x\partial y},\tag{24}$$

$$E=\frac{\partial\Psi}{\partial y}-\delta\left(\frac{\partial\Psi}{\partial y}\frac{\partial\phi}{\partial x}-\frac{\partial\Psi}{\partial x}\frac{\partial\phi}{\partial y}\right)+\frac{1}{Rm}\left(\delta^2\,\frac{\partial^2}{\partial x^2}+\frac{\partial^2}{\partial y^2}\right)\phi,\tag{25}$$

$$\begin{aligned}2\delta\,\frac{\partial^2\Psi}{\partial x\partial y}&=S_{xx}+We\,\delta\left(\frac{\partial\Psi}{\partial y}\frac{\partial}{\partial x}-\frac{\partial\Psi}{\partial x}\frac{\partial}{\partial y}\right)S_{xx}-\\&\quad 2e\delta We\,\frac{\partial^2\Psi}{\partial x\partial y}-2\,\frac{\partial^2\Psi}{\partial y^2}S_{xy}-We\left(\delta^2(1-e)\,\frac{\partial^2\Psi}{\partial x^2}+(1+e)\,\frac{\partial^2\Psi}{\partial y^2}\right)S_{xy},\end{aligned}\tag{26}$$

$$\begin{aligned}\left(\frac{\partial^2\Psi}{\partial y^2}-\delta^2\,\frac{\partial^2\Psi}{\partial x^2}\right)&=S_{xy}+We\,\delta\left(\frac{\partial\Psi}{\partial y}\frac{\partial}{\partial x}-\frac{\partial\Psi}{\partial x}\frac{\partial}{\partial y}\right)S_{xy}+\\&\quad\frac{We}{2}\left((1-e)\,\frac{\partial^2\Psi}{\partial y^2}+\delta^2(1+e)\,\frac{\partial^2\Psi}{\partial x^2}\right)S_{xx}-\\&\quad\frac{We}{2}\left((1+e)\,\frac{\partial^2\Psi}{\partial y^2}+\delta^2(1-e)\,\frac{\partial^2\Psi}{\partial x^2}\right)S_{yy},\end{aligned}\tag{27}$$

$$\begin{aligned}-2\delta\,\frac{\partial^2\Psi}{\partial x\partial y}&=S_{yy}+We\,\delta\left(\frac{\partial\Psi}{\partial y}\frac{\partial}{\partial x}-\frac{\partial\Psi}{\partial x}\frac{\partial}{\partial y}\right)S_{yy}+\\&\quad 2e\delta WeS_{yy}\,\frac{\partial^2\Psi}{\partial x\partial y}+We\left((1-e)\,\frac{\partial^2\Psi}{\partial y^2}+\delta^2(1+e)\,\frac{\partial^2\Psi}{\partial x^2}\right)S_{xy},\end{aligned}\tag{28}$$

其中,连续方程(3)得到自动满足,$\delta$,$We$,$Re$,$Rm$,$S$ 和 $Ha$ 分别为波数、Weissenberg 数、Reynolds 数、磁场 Reynolds 数、Stommer 数和 Hartman 数,$p_{\mathrm{m}}$ 为总压力,由常规压力和磁场压力组成,$E$ 为电场强度,$\alpha=b/a$ 为波幅比,$\Psi$ 为流函数,$\phi$ 为磁力函数.

采用长波长和低 Reynolds 数假定,方程(23)~(28)变为

$$\left(\frac{\mu+\eta}{\eta}\right)\frac{\partial p}{\partial x}=\frac{\partial S_{xy}}{\partial y}+\frac{\mu}{\eta}\,\frac{\partial^3\Psi}{\partial y^3}+ReS^2\,\frac{\partial^2\phi}{\partial y^2},\tag{29}$$

$$\left(\frac{\mu+\eta}{\eta}\right)\frac{\partial p}{\partial y}=0,\tag{30}$$

$$E=\frac{\partial\Psi}{\partial y}+\frac{1}{Rm}\,\frac{\partial^2\phi}{\partial y^2},\tag{31}$$

$$S_{xx}-We(1+e)\,\frac{\partial^2\Psi}{\partial y^2}S_{xy}=0,\tag{32}$$

$$\frac{\partial^2\Psi}{\partial y^2}=S_{xy}+\frac{We}{2}(1-e)\,\frac{\partial^2\Psi}{\partial y^2}S_{xx}-\frac{We}{2}(1+e)\,\frac{\partial^2\Psi}{\partial y^2}S_{yy},\tag{33}$$

$$S_{yy}+We(1-e)\,\frac{\partial^2\Psi}{\partial y^2}S_{xy}=0.\tag{34}$$

方程(30)表明 $p$ 不是 $y$ 的函数,因此 $p=p(x)$. 由方程(29)、(30)和(32)~(34)可以得到

$$\frac{\partial^2}{\partial y^2}S_{xy}+\frac{\partial^4\Psi}{\partial y^4}-Ha^2\,\frac{\partial^2\Psi}{\partial y^2}=0,\tag{35}$$

$$S_{xy}=\frac{\partial^2\Psi/\partial y^2}{1+We^2(1-e^2)\,(\partial^2\Psi/\partial y^2)^2}.\tag{36}$$

相应的边界条件为

$$\frac{\partial\Psi}{\partial y}+\beta\left[\frac{\partial^2\Psi}{\partial y^2}+S_{xy}\right]=-1,\qquad y=h(x),\tag{37}$$

$$\begin{cases} \Psi = 0,\ \dfrac{\partial^2 \Psi}{\partial y^2} = 0,\ \dfrac{\partial \phi}{\partial y} = 0, & y = 0, \\ \Psi = F,\ \phi = 0, & y = h(x), \end{cases} \tag{38}$$

$$F = \int_0^h \frac{\partial \Psi}{\partial y}\,\mathrm{d}y,\ \theta = F + 1, \tag{39}$$

其中,$\beta$ 为无量纲壁面滑移参数,$\theta$ 和 $F$ 分别表示实验室坐标系和波动坐标系中的无量纲平均流量比.

应用二项展开式,方程(29)和(35)~(37)可以表示为

$$\frac{\partial^2}{\partial y^2}\left(\frac{\partial^2 \Psi}{\partial y^2} - Ha^2 \frac{\eta}{\mu + \eta}\Psi\right) + We^2\alpha_1\left(\frac{\partial^2 \Psi}{\partial y^2}\right)^3 + We^4\alpha_2\left(\frac{\partial^2 \Psi}{\partial y^2}\right)^5 = 0, \tag{40}$$

$$\frac{\partial p}{\partial x} = \frac{\partial^3 \Psi}{\partial y^3} + Ha^2 \frac{\eta}{\mu + \eta}\left(E - \frac{\partial \Psi}{\partial y}\right) + We^2\alpha_1 \frac{\partial}{\partial y}\left(\frac{\partial^2 \Psi}{\partial y^2}\right)^3 + We^4\alpha_2 \frac{\partial}{\partial y}\left(\frac{\partial^2 \Psi}{\partial y^2}\right)^5, \tag{41}$$

$$\frac{\partial \Psi}{\partial y} + \beta\left[\frac{\partial^2 \Psi}{\partial y^2}\left(1 - We^2(1 - e^2)\left(\frac{\partial^2 \Psi}{\partial y^2}\right)^2 + We^4(1 - e^2)\left(\frac{\partial^2 \Psi}{\partial y^2}\right)^4\right)\right] = -1, \quad y = h(x), \tag{42}$$

其中

$$\alpha_1 = \frac{(e^2 - 1)\eta}{\eta + \mu},\ \alpha_2 = (e^2 - 1)\alpha_1,\ \xi = \frac{\eta}{\mu + \eta}.$$

## 2　解 表 达 式

将表达式

$$\psi = \psi_0 + We^2\psi_1 + We^4\psi_2 + \cdots, \tag{43}$$

$$\frac{\mathrm{d}p}{\mathrm{d}x} = \frac{\mathrm{d}p_0}{\mathrm{d}x} + We^2 \frac{\mathrm{d}p_1}{\mathrm{d}x} + We^4 \frac{\mathrm{d}p_2}{\mathrm{d}x} + \cdots, \tag{44}$$

$$\phi = \phi_0 + We^2\phi_1 + We^4\phi_2 + \cdots, \tag{45}$$

$$F = F_0 + We^2F_1 + We^4F_2\cdots \tag{46}$$

代入上述方程(31)和(38)~(42),并解之直到 $O(We^4)$,连同下式一起

$$F_0 = F - We^2F_1 - We^4F_2, \tag{47}$$

我们就可以得到

$$\begin{aligned} \Psi = {} & \frac{C_0}{2}(\cosh(Ha\,y\sqrt{\xi}) + \sinh(Ha\,y\sqrt{\xi}))C_1(y) + \\ & We^2\left\{\frac{C_0^4}{64}(F + 2h)^3Ha^4\alpha_1\xi^2(\cosh(3Ha\,y\sqrt{\xi}) - \sinh(3Ha\,y\sqrt{\xi}))\sum_{i=2}^{3} C_i(y)\right\} + \\ & We^4\left\{\frac{C_0^7}{6\ 144}(\cosh(5Ha\,y\sqrt{\xi}) - \sinh(5Ha\,y\sqrt{\xi}))(F + 2h)^5Ha^8\xi^4\sum_{i=4}^{18} C_i(y)\right\}, \end{aligned} \tag{48}$$

$$\begin{aligned} \phi = {} & \frac{Rm}{4Ha\sqrt{\xi}}(\cosh(Ha\,y\sqrt{\xi}) + \sinh(Ha\,y\sqrt{\xi}))L_1(y) + \\ & We^2\left\{\frac{-RmC_0^4}{192}(F + 2h)^3Ha^3\xi^{3/2}\alpha_1(\cosh(3Ha\,y\sqrt{\xi}) - \right. \end{aligned}$$

$$\sinh(3Ha\,y\sqrt{\xi}))\sum_{j=2}^{4}L_j(y)\Big\}+$$

$$We^4\Big\{\frac{-RmC_0^7}{30\,720}(F+2h)^5Ha^7\xi^{7/2}(\cosh(5Ha\,y\sqrt{\xi})-$$

$$\sinh(5Ha\,y\sqrt{\xi}))\sum_{j=5}^{25}L_j(y)\Big\}, \tag{49}$$

其中，$C_i(i=1,\cdots,18)$ 和 $L_j(j=1,\cdots,25)$ 按常规做法得到.

压力梯度 $\mathrm{d}p/\mathrm{d}x$、压力增量 $\Delta P_\lambda$、轴向感应磁场 $h_x$ 和电流密度 $J_z$ 分别如下给出：

$$\frac{\mathrm{d}p}{\mathrm{d}x}=\frac{\partial^3\Psi}{\partial y^3}+Ha^2\xi\left(E-\frac{\partial\Psi}{\partial y}\right)+We^2\alpha_1\frac{\partial}{\partial y}\left(\frac{\partial^2\Psi}{\partial y^2}\right)^3+We^4\alpha_2\frac{\partial}{\partial y}\left(\frac{\partial^2\Psi}{\partial y^2}\right)^5, \tag{50}$$

$$\Delta P_\lambda=\int_0^1\left(\frac{\mathrm{d}p}{\mathrm{d}x}\right)_{y=0}\mathrm{d}x, \tag{51}$$

$$h_x=\frac{\partial\phi}{\partial y}, \tag{52}$$

$$J_z=-\frac{\partial h_x}{\partial y}. \tag{53}$$

## 3 讨　论

J-S 流体为肠道和小血管中蠕动运动提供了一个良好的理解模型. 小肠中的食糜是 J-S 流体的一个样例，血液也呈现出小直径管道中低剪切率非 Newton 流体的流动特性. 该流体模型展现出肉眼可见的壁面滑移. 这种状况相当于滑移流动，壁面上流体的粘合力较小，流体滑过壁面. 本节强调壁面滑移参数 $\beta$、Weissenberg 数 $We$、磁场 Reynolds 数 $Rm$ 和 Hartman 数 $Ha$，对 $\psi$，$\mathrm{d}p/\mathrm{d}x$，$\Delta P_\lambda$，$u$，$h_x$ 和 $J_z$ 的影响.

### 3.1 泵的特性

图 1(a) ~ (c)描述了 $We$，$\beta$ 和 $Ha$ 取不同数值时，$\mathrm{d}p/\mathrm{d}x$ 随 $x$ 的变化. 从图 1(a)可以发现，在通道宽 $x\in[0,0.5]$ 和 $x\in[1,1.2]$ 区域，压力梯度相对较小，意味着流动可以很容易通过，而无需承受多大的压力梯度. 在通道 $x\in[0.5,1]$ 的狭窄区域，需要较大的压力梯度维持流量通过该狭窄部分管道. 需要注意的是，当 $We$ 值增大时，压力梯度在减小. 进一步地，图 1(b)和图 1(c)显示，$\mathrm{d}p/\mathrm{d}x$ 是 $\beta$ 的减函数，而是 $Ha$ 的增函数.

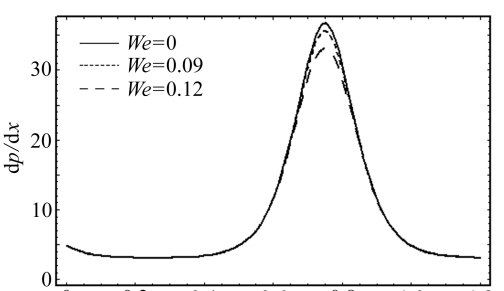


(a) $e=0.8$, $\beta=0.1$, $E=2.5$, $Ha=1.5$, $\alpha=0.3$, $\mu=1$, $\theta=0.1$, $\eta=1$

当 $We$，$\beta$ 和 $Ha$ 取不同数值时，压力增量 $\Delta P_\lambda$ 随着平均流量比 $\theta$ 的变化在图 2(a) ~ (c)中绘出. 图 2(a)清楚地表明，在增压泵区 ($\Delta P_\lambda>0$)，压力增量随着 $We$ 的增大而减小；在零增压区 ($\Delta P_\lambda=0$)，Weissenberg 数 $We$ 对压力增量没有影响；在负增压区 ($\Delta P_\lambda<0$)，负增压随着 $We$ 的增大而增大. 图 2(b)显示，$\beta$ 对 $\Delta P_\lambda$ 的影响与 $We$ 相类似，但前者没有零增压区. 与滑移参数 $\beta$ 相比较，Hartman 数 $Ha$ 对压力增量 $\Delta P_\lambda$ 的影响正相反(见图 2(c)).

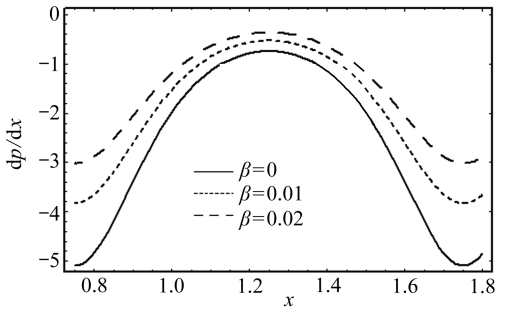


(b) $e=0.8$, $We=0.05$, $E=2.5$, $Ha=1.5$, $\alpha=0.3$, $\mu=0.51$, $\theta=0.1$, $\eta=0.1$

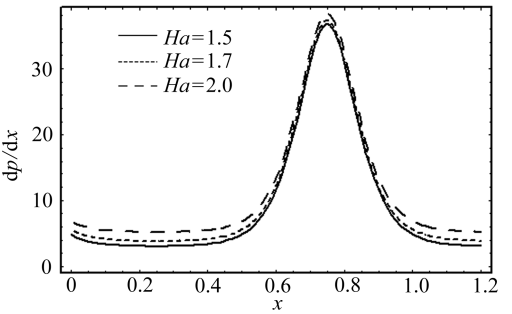


(c) $e=0.8$, $We=0.01$, $E=2.5$, $\beta=0.1$, $\alpha=0.6$, $\mu=1$, $\theta=-3.5$, $\eta=1$

**图1**　压力梯度 $dp/dx$ 随 $x$ 的变化

Fig. 1　The pressure gradient $dp/dx$ versus $x$

## 3.2　流动特性

图3(a)~(c)描述出流动参数对纵向速度 $u$ 的影响.需要注意的是,某些参数的变化,对通道中心和壁面附近的影响是不同的,在通道中心线 $y=0$ 处出现最大的不一致.从图3(a)和图3(c)可以发现, $We$ 和 $Ha$ 对通道中心线处速度的影响正相反.图3(b)表明,在通道的中心线上,速度的值随着 $\beta$ 的增大而增大,受滑移的影响,壁面处的速度曲线在上升.根据 Navier 条件:壁面上的滑移量与壁面上的剪切应力成线性比例.因此,期待在微循环血液流动的研究中,滑移条件得到有益的生理学应用.

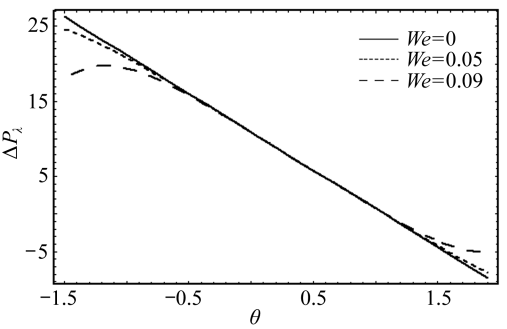


(a) $e=0.8$, $\beta=0.05$, $E=1$, $Ha=3.5$, $\alpha=0.6$, $\mu=1$, $\eta=1$

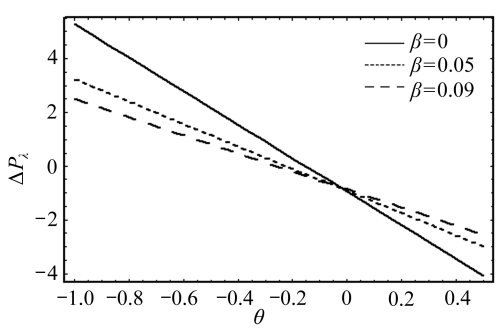


(b) $e=0.8$, $We=0.01$, $E=-1$, $Ha=1.5$, $\alpha=0.6$, $\mu=1$, $\eta=1$

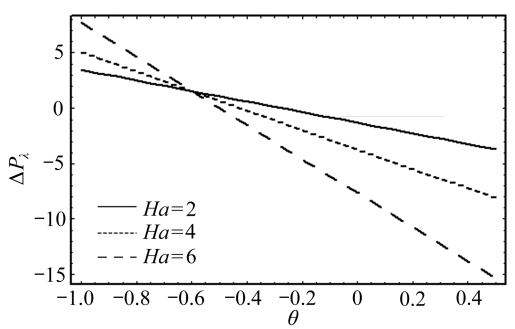


(c) $e=0.8$, $We=0.01$, $E=-1$, $\beta=0.05$, $\alpha=0.6$, $\mu=1$, $\eta=1$

**图2**　压力增量 $\Delta P_\lambda$ 随着平均流量比 $\theta$ 的变化

Fig. 2　The pressure rise $\Delta P_\lambda$ against flow rate $\theta$

## 3.3　磁场特性

毫无疑问,血液是最典型的生物磁流体.在磁场作用下的、壁面无摩擦的平行板状通道中,可以洞悉血液流动特性的机理.当 $We$,$\beta$,$Ha$ 和 $Rm$ 取不同数值时,轴向感应磁场 $h_x$ 随 $y$ 的变化绘于图4(a)~(d).显然,在左半边区域,轴向感应磁场 $h_x$ 方向相同;与右半边区域,轴向感应

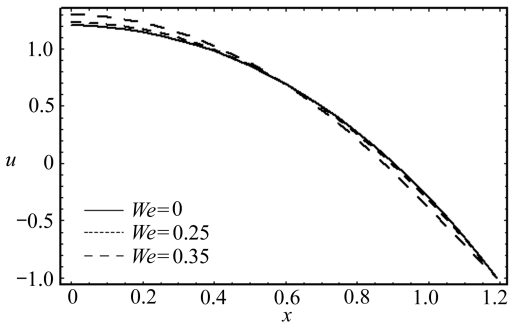


(a) $e=0.8$, $E=1$, $x=0.2$, $\beta=0.001$, $\theta=2.2$, $\alpha=0.2$, $\mu=0.5$, $\eta=0.1$

磁场 $h_x$ 的方向正相反. $y=0$ 处轴向感应磁场 $h_x$ 等于 0 的条件,可以作为磁力函数 $\phi$ 的边界条件. 图 4(a) ~ (c)表明, $h_x$ 的绝对值随着 $We$,$\beta$ 和 $Ha$ 的增大而减小. $h_x$ 的绝对值随着 $Rm$ 的增大而增大(见图 4(d)).

当 $Rm$,$\beta$,$We$ 和 $Ha$ 取不同数值时,图 5(a) ~ (d)绘出了电流密度 $J_z$ 随 $y$ 的分布曲线. 可以发现,曲线都呈自然抛物线. 对 $y$ 的某个区域,随着 $J_z$ 值从增大走向减小,都将导致通道中净余电流为 0 的物理事实. 此外,与邻近壁面处相比较,通道中心处参数的行为明显不同. 需要指出的是,从

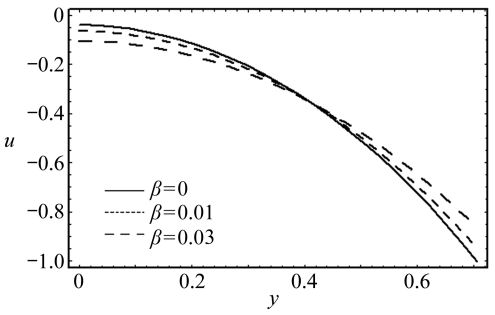


(b) $e=0.3$, $E=1$, $We=0.05$, $x=0.2$, $\theta=2$, $Ha=1.5$, $\alpha=0.2$, $\mu=0.5$, $\eta=0.1$

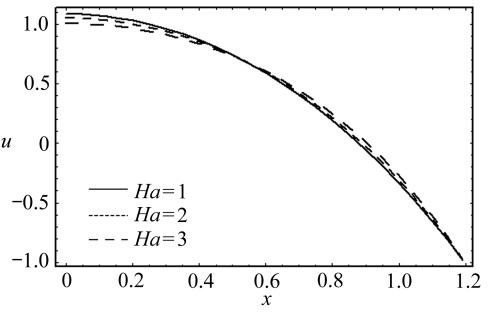


(c) $e=0.8$, $E=1$, $We=0.05$, $x=0.2$, $\theta=2$, $\beta=0.001$, $\alpha=0.2$, $\mu=0.5$, $\eta=0.1$

**图 3** 轴向速度 $u$ 随 $y$ 的变化

Fig. 3 Axial velocity $u$ versus $y$

图 5(a) ~ (c)可以看到,通道中心处的 $J_z$ 值随着 $We$,$\beta$ 和 $Ha$ 的增大而减小,而在通道壁面附近范围内,$J_z$ 反而在增大. 图 5(d)显示,通道中心处的电流密度 $J_z$, 是磁场 Reynolds 数 $Rm$ 的增函数.

### 3.4 俘获现象

图 6 ~ 8 研究了俘获现象. 通常, 流线的形状几乎都是顺着界面分布的, 但是在某些条件

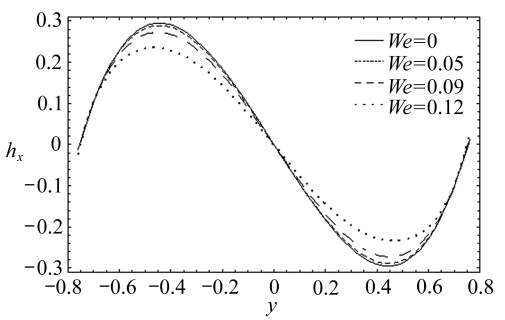


(a) $e=0.8$, $E=1$, $Ha=2.5$, $Rm=1$, $x=-0.2$, $\theta=2.3$, $\beta=0.001$, $\alpha=0.3$, $\mu=0.5$, $\eta=0.5$

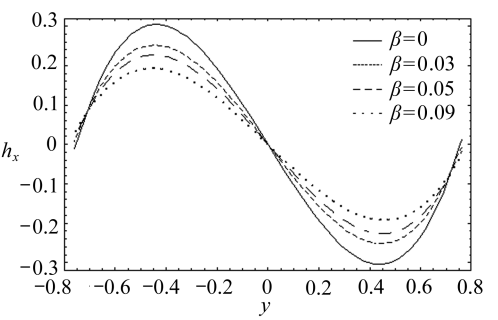


(b) $e=0.8$, $E=1$, $Ha=1.5$, $Rm=1$, $x=-0.2$, $\theta=2.3$, $We=0.01$, $\alpha=0.3$, $\mu=0.5$, $\eta=0.5$

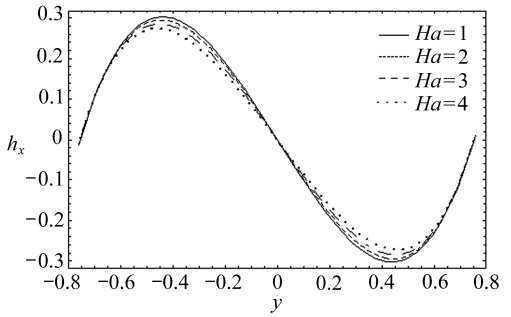


(c) $e = 0.8$, $E = 1$, $\beta = 0.01$, $Rm = 1$, $x = -0.2$, $\theta = 2.3$, $We = 0.01$, $\alpha = 0.3$, $\mu = 0.5$, $\eta = 0.5$

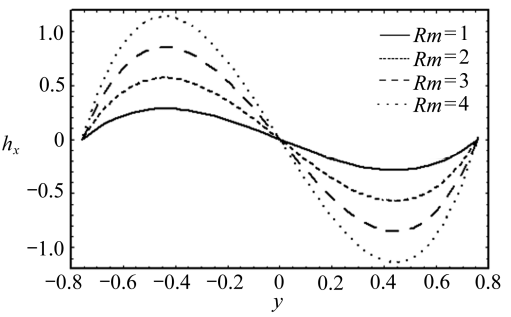


(d) $e = 0.1$, $E = 0.8$, $\beta = 0.01$, $Ha = 1.5$, $x = -0.2$, $\theta = 2.3$, $We = 0.01$, $\alpha = 0.3$, $\mu = 0.5$, $\eta = 0.5$

**图 4**　轴向感应磁场 $h_x$ 随 $y$ 的变化

Fig. 4　Axial induced magnetic field $h_x$ versus $y$

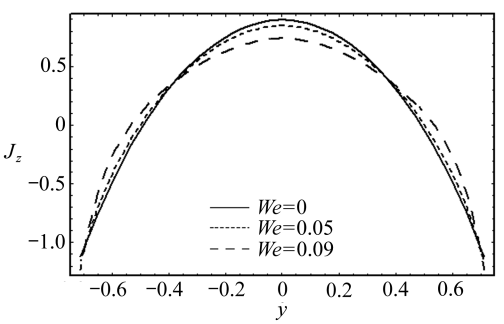


(a) $e = 0.2$, $E = 0.8$, $\beta = 0.05$, $Ha = 1.7$, $x = -0.2$, $\theta = 2.5$, $Rm = 1$, $\alpha = 0.3$, $\mu = 0.5$, $\eta = 0.5$

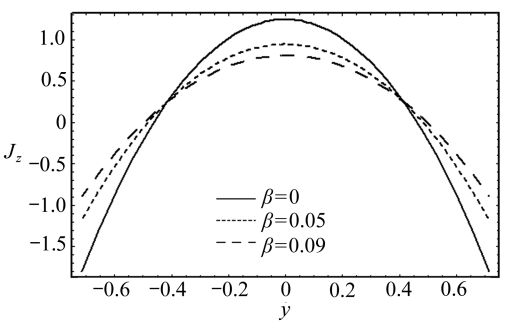


(b) $e = 0.1$, $E = 0.8$, $Rm = 1$, $Ha = 1.7$, $x = -0.2$, $\theta = 2.5$, $We = 0.03$, $\alpha = 0.3$, $\mu = 0.5$, $\eta = 0.5$

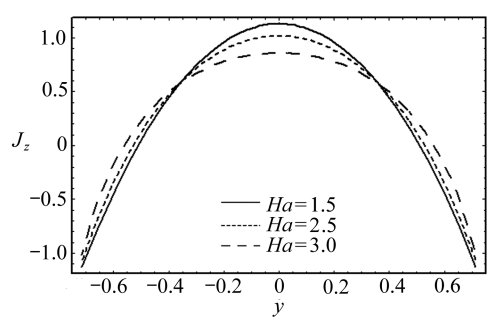


(c) $e = 0.1$, $E = 0.8$, $Rm = 1$, $\beta = 0.05$, $x = -0.2$, $\theta = 2.5$, $We = 0.03$, $\alpha = 0.3$, $\mu = 0.5$, $\eta = 0.5$

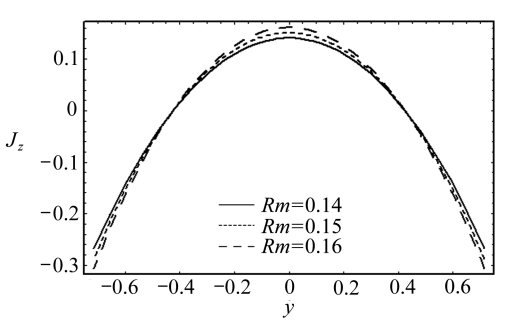


(d) $e = 0.1$, $E = 1$, $Ha = 1.5$, $\beta = 0.05$, $x = -0.2$, $\theta = 2.5$, $We = 0.03$, $\alpha = 0.3$, $\mu = 0.5$, $\eta = 0.5$

**图 5**　电流密度 $J_z$ 随 $y$ 的变化

Fig. 5　Current density $J_z$ versus $y$

下,会分离出闭合的循环流线.一些流体以这样的一种方式:成群地围在闭合流线的中心区域.闭合流线构成一个流体团块,它们作为一个整体以波阵面形式向前移动.这可能就是血液中的红细胞在血管轴线附近聚集,而血浆向血管壁迁移的原因.图 6 和图 8 显示,流体团块的体积随着 $We$ 和 $Ha$ 的增大而缩小.而俘获流体团块的大小随着 $\beta$ 的增大而减小(见图 7).

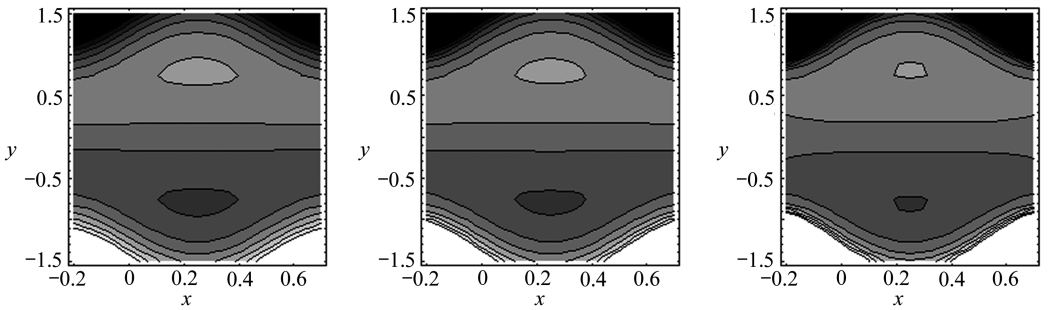


(a) $We = 0$ (b) $We = 0.5$ (c) $We = 0.6$

**图 6** 不同 $We$ 值对应的流线图(其他参数为 $e = 0.8$, $E = 1$, $Ha = 1.9$, $\beta = 0.01$, $\theta = 1.1$, $\alpha = 0.3$, $\mu = 1$, $\eta = 1$)

Fig. 6 Streamlines for variable value of $We$ (the other parameters are $e = 0.8$, $E = 1$, $Ha = 1.9$, $\beta = 0.01$, $\theta = 1.1$, $\alpha = 0.3$, $\mu = 1$, $\eta = 1$)

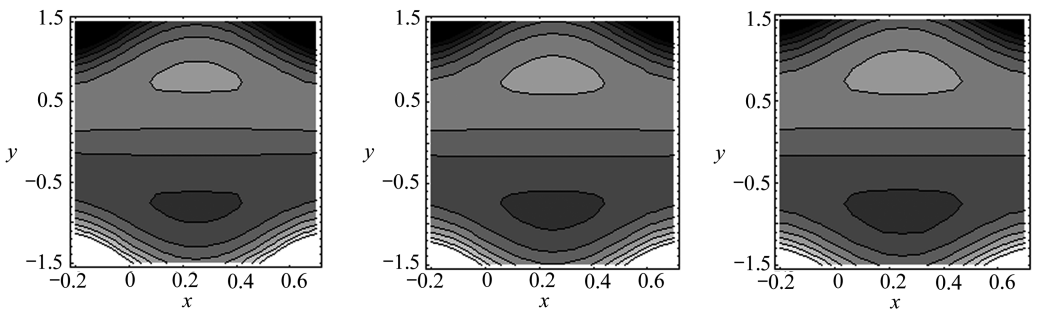


(a) $\beta = 0$ (b) $\beta = 0.5$ (c) $\beta = 0.6$

**图 7** 不同 $\beta$ 值对应的流线图(其他参数为 $e = 0.8$, $E = 1$, $Ha = 1.5$, $We = 0.01$, $\theta = 1.2$, $\alpha = 0.3$, $\mu = 1$, $\eta = 1$)

Fig. 7 Streamlines for variable value of $\beta$ (the other parameters are $e = 0.8$, $E = 1$, $Ha = 1.5$, $We = 0.01$, $\theta = 1.2$, $\alpha = 0.3$, $\mu = 1$, $\eta = 1$)

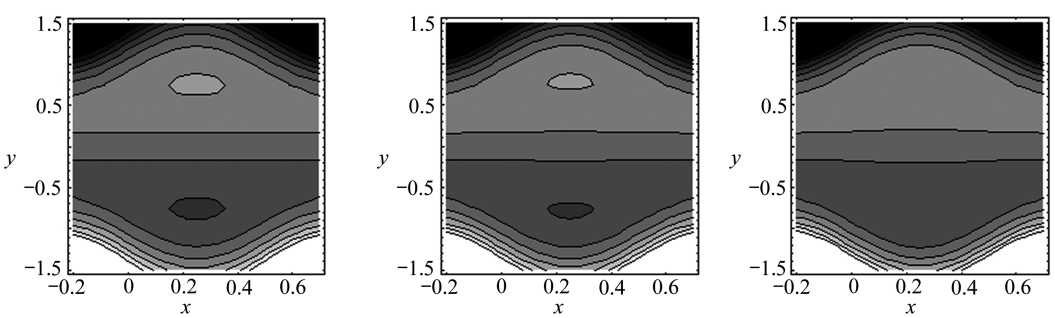


(a) $Ha = 1.5$ (b) $Ha = 2.5$ (c) $Ha = 3.5$

**图 8** 不同 $Ha$ 值对应的流线图(其他参数为 $e = 0.8$, $E = 1$, $\beta = 0.01$, $\theta = 1$, $\alpha = 0.3$, $\mu = 1$, $\eta = 1$)

Fig. 8 Streamlines for variable value of $Ha$ (the other parameters are $e = 0.8$, $E = 1$, $\beta = 0.01$, $\theta = 1$, $\alpha = 0.3$, $\mu = 1$, $\eta = 1$)

## 4 结　　语

研究了感应磁场对 Johnson-Segalman(J-S)流体蠕动流的影响. 解析地得到流函数、磁力函数、轴向压力梯度、轴向感应磁场和电流密度的摄动表达式. 给出了单位波长的压力增量、轴向感应磁场、电流密度和俘获流体团的图形结果. 主要结论可归纳如下:

1）与 Newton 流体相比,J-S 流体的轴向压力梯度 $dp/dx$ 值较小;

2）在增压泵区,J-S 流体比 Newton 流体,单位波长的压力增量值较小,而当流量达到一定数值时,Newton 流体和 J-S 流体间没有什么区别;

3）Newton 流体的轴向感应磁场,高于 J-S 流体的轴向感应磁场;

4）磁场 Reynolds 数会增大轴向感应磁场;

5）通道中心处 Newton 流体的电流密度 $J_z$, 比 J-S 流体的电流密度要大;

6）如果按 Newton 流体到 J-S 流体排列,通道中心处所俘获流体团块的大小在增大.

**致谢**　本文工作也得到沙特阿拉伯阿卜杜勒-阿齐兹国王大学科学研究院(DSR)的支持,在此表示感谢.

## 参考文献(References):

[1] Latham T W. *Fluid Motion in a Peristaltic Pump*[M]. MIT Cambridge MA, 1966.

[2] Shapiro A H, Jaffrin M Y, Weinberg S L. Peristaltic pumping with long wavelength at low Reynolds number[J]. *J Fluid Mech*, 1969, **37**: 799-825.

[3] Mekheimer Kh S, Abdelmaboud Y. The influence of heat transfer and magnetic field on peristaltic transport of a Newtonian fluid in a vertical annulus: application of an endoscope[J]. *Phys Lett A*, 2008, **372**(10): 1657-1665.

[4] Mekheimer Kh S. Peristaltic flow of blood under effect of a magnetic field in a non-uniform channels[J]. *Appl Math Comput*, 2004, **153**(3): 763-777.

[5] Mekheimer Kh S, Abdelmaboud Y. Peristaltic flow of a couple stress fluid in an annulus: application of an endoscope[J]. *Physica A*, 2008, **387**(11): 2403-2415.

[6] Vajravelu K, Radhakrishnamacharya G, Murty V R. Peristaltic flow and heat transfer in a vertical porous annulus, with long wave approximation[J]. *Int J Nonlinear Mech*, 2007, **42**(5): 754-759.

[7] Vajravelu K, Sreenadh S, Babu V R. Peristaltic pumping of a Herschel-Bulkley fluid in a channel[J]. *Appl Math Comput*, 2005, **169**(1): 726-735.

[8] Kothandapani M, Srinivas S. Peristaltic transport of a Jeffrey fluid under the effect of magnetic field in an asymmetric channel[J]. *Int J Nonlinear Mech*, 2008, **43**(9): 915-924.

[9] Kothandapani M, Srinivas S. On the influence of wall properties in the MHD peristaltic transport with heat transfer and porous medium[J]. *Phys Lett A*, 2008, **372**(25): 4586-4591.

[10] Kothandapani M, Srinivas S. Nonlinear peristaltic transport of a Newtonian fluid in an inclined asymmetric channel through a porous medium[J]. *Phys Lett A*, 2008, **372**(8): 1265-1276.

[11] Haroun M H. Effect of Deborah number and phase difference on peristaltic transport of a third order fluid in an asymmetric channel[J]. *Comm Nonlinear Sci Numer Simul*, 2007, **12**(8): 1464-1480.

[12] Haroun M H. Non-linear peristaltic flow of a fourth grade fluid in an inclined asymmetric channel[J]. *Comput Mater Sci*, 2007, **39**(2): 324-333.

[13] Eldabe N T M, Al-Sayad M F, Galy A Y, Sayed H M. Peristaltically induced transport of a MHD biviscosity fluid in a non-uniform tube[J]. *Physica A*, 2007, **383**(2): 253-266.

[14] Nadeem S, Akram S. Peristaltic flow of a Williamson fluid in an asymmetric channel[J]. *Comm Nonlinear Sci Numer Simul*, 2010, **15**(7): 1705-1716.

[15] Ali N, Hayat T. Peristaltic flow of a micropolar fluid in an asymmetric channel[J]. *Comp Math Applications*, 2008, **55**(4): 589-608.

[16] Hayat T, Ali N, Asghar S, Siddiqui A M. Exact peristaltic flow in tubes with an endoscope [J]. *Appl Math Comput*, 2006, **182**(1): 359-368.

[17] Hayat T, Ali N. Effect of variable viscosity on the peristaltic transport of a Newtonian fluid in an asymmetric channel[J]. *Appl Math Model*, 2008, **32**(5): 761-774.

[18] Wang Y, Hayat T, Ali N, Oberlack M. Magnetohydrodynamic peristaltic motion of a Sisko fluid in a symmetric or asymmetric channel[J]. *Physica A*, 2008, **387**(2/3): 347-362.

[19] Hayat T, Ali N. A mathematical description of peristaltic hydromagnetic flow in a tube[J]. *Appl Math Comput*, 2007, **188**(2): 1491-1502.

[20] Hayat T, Khan M, Siddiqui A M, Asghar S. Non-linear peristaltic flow of a non-Newtonian fluid under effect of a magnetic field in a planar channel[J]. *Comm Nonlinear Sci Numer Simul*, 2007, **12**(6): 910-919.

[21] Ebaid E. Effects of magnetic field and wall slip conditions on the peristaltic transport of a Newtonian fluid in an asymmetric channel[J]. *Phys Lett A*, 2008, **372**(24): 4493-4499.

[22] Srinivas S, Gayathri R, Kothandapani M. The influence of slip conditions, wall properties and heat transfer on the MHD peristaltic transport[J]. *Comp Phys Comm*, 2009, **180**(11): 2115-2122.

[23] Mandviwalla X, Archer R. The influence of slip boundary conditions on the peristaltic pumping in a rectangular channel[J]. *J Fluids Eng*, 2008,**130**(12): 124501-124505.

[24] El-Shehawy E, El- Dabe N, El-Desoky I. Slip effects on the peristaltic flow of a non-Newtonian Maxwellian fluid[J]. *Acta Mechanica*, 2006, **186**(1/4): 141-159.

[25] Sobh A M. Interection of couple stresses and slip flow on peristaltic transport in uniform and nonuniform channels[J]. *Turkish J Eng Env Sci*, 2008, **32**(2):117-123.

[26] Hayat T, Hussain Q, Ali N. Influence of partial slip on the peristaltic flow in a porous medium[J]. *Phys Lett A*, 2008, **387**(14): 3399-3409.

[27] Ali N, Hussain Q, Hayat T, Asghar S. Slip effects on the peristaltic transport of MHD fluid with variable viscosity[J]. *Phys Lett A*, 2008, **372**(9): 1477-1489.

[28] Hayat T, Hina S, Ali N. Simultaneous effects of slip and heat transfer on the peristaltic flow [J]. *Comm Nonlinear Sci Numer Simul*, 2010, **15**(6): 1526-1537.

[29] Hayat T, Qureshi M U, Ali N. The influence of slip on the peristaltic motion of a third order fluid in an asymmetric channel[J]. *Phys Lett A*, 2008, **372**(15): 2653-2664.

[30] Vishnyakov V I, Pavlov K B. Peristaltic flow of a conductive liquid in a transverse magnetic field[J]. *Translated From Magnitnaya Gidrodinamika*, 1972, **8**(2): 174-178.

[31] Mekheimer Kh S. Effect of the induced magnetic field on peristaltic flow of a couple stress fluid[J]. *Phys Lett A*, 2008, **372**(23): 4271-4278.

[32] Nadeem S, Akram S. Peristaltic flow of a couple stress fluid under the effect of induced magnetic field in an asymmetric channel[J]. *Arch Appl Mech*, 2011, **81**(1): 97-109.

[33] Hayat T, Khan Y, Ali N, Mekheimer Kh S. Effect of an induced magnetic field on the peristaltic flow of a third order fluid[J]. *Numer Methods Partial Diff Eqs*, 2010, **26**(2): 345-366.

[34] Hayat T, Saleem N, Ali N. Effect of induced magnetic field on peristaltic transport of a Carreau fluid[J]. *Comm Nonlinear Sci Numer Simul*, 2010,**15**(9):2407-2423.

[35] Mekheimer Kh S. Peristaltic flow of a magneto-micropolar fluid: effect of induced magnetic field[J]. *J Appl Math*, 2008,**2008**:570825-570848.

# Slip and Induced Magnetic Field Effects on the Peristaltic Transport of a Johnson-Segalman Fluid

T. Hayat[1], S. Noreen[2], A. Alsaedi[3]

(1. *Department of Mathematics*, *Quaid-I-Azam University* 45320, *Islamabad* 44000, *Pakistan*;
2. *Department of Mathematics*, *Comsats Institute of Information Technology*, *Attock* 43600, *Pakistan*;
3. *Department of Mathematics*, *Faculty of Science*, *King Adbulaziz University*, *Jeddah* 21589, *Saudi Arabia*)

**Abstract**: Peristaltic flow of a Johnson-Segalman fluid in a planar channel was investigated in the presence of an induced magnetic field and slip condition. Symmetric nature of flow in a channel was adopted. The velocity slip condition in terms of shear stress was taken into account. Mathematical formulation was first presented and then the subjected equations were solved under the long wavelength and low Reynolds number approximations. Perturbations solutions were established for the pressure rise, axial velocity, microrotation component, stream function, magnetic-force function, axial induced magnetic field, and current distribution across the channel. Solution expressions for small Weissenberg number were derived. The flow quantities of interest were sketched and analyzed.

**Key words**: induced magnetic field; slip condition; Johnson-Segalman fluid